

# Homozygosity for a Novel *ABCA4* Founder Splicing Mutation Is Associated with Progressive and Severe Stargardt-like Disease

Anat Beit-Ya'acov,<sup>1</sup> Liliana Mizrahi-Meissonnier,<sup>1</sup> Alexey Obolensky,<sup>1</sup> Carmit Landau,<sup>2</sup> Anat Blumenfeld,<sup>1</sup> Ada Rosenmann,<sup>2</sup> Eyal Banin,<sup>1,3</sup> and Dror Sharon<sup>1,3</sup>

**PURPOSE.** To clinically characterize and genetically analyze members of six families who reside in the same village and manifest a rare form of retinal degeneration.

**METHODS.** Ophthalmic evaluation included a full clinical examination, perimetry, color vision testing, and electroretinography. Genomic DNA was screened for *ABCA4* mutations with the use of microarray analysis and direct sequencing. RNA analysis was performed with RT-PCR and sequencing.

**RESULTS.** The authors recruited 15 patients with a unique retinal disease who are members of six highly consanguineous Arab-Muslim families from a single village. During early stages of disease, funduscopic and angiographic findings as well as retinal function resemble those of Stargardt disease. However, later in life, severe, widespread cone-rod degeneration ensues. Marked progressive involvement of the retinal periphery distinguishes this phenotype from classic Stargardt disease. Genetic analysis of *ABCA4* revealed two novel deletions, p.Cys1150del and c.4254-15del23. One patient, who was a compound heterozygote, manifested typical Stargardt disease. The remaining 14 patients were homozygote for the c.4254-15del23 intronic deletion and had the progressive form of disease. We identified an identical *ABCA4* haplotype in all alleles carrying this mutation, indicating a founder mutation. Detailed RT-PCR analysis in normal retina and lymphoblastoid cells revealed expression of the full-length *ABCA4* transcript and three novel transcripts produced by alternative splicing. The full-length *ABCA4* transcript, however, could not be detected in lymphoblastoid cells of affected homozygote patients.

**CONCLUSIONS.** These results expand the genotype-phenotype correlation of *ABCA4*, showing that homozygosity for the novel c.4254-15del23 splicing mutation is associated with a severe progressive form of disease. (*Invest Ophthalmol Vis Sci* 2007;48:4308–4314) DOI:10.1167/iovs.07-0244

From the <sup>1</sup>Department of Ophthalmology, Hadassah-Hebrew University Medical Center, Jerusalem, Israel; and the <sup>2</sup>Michaelson Institute for vision rehabilitation, Hadassah-Hebrew University Medical Center, Jerusalem, Israel.

<sup>3</sup>These authors contributed equally to the work presented here and should therefore be regarded as equivalent authors.

Supported by the American Health Assistance Foundation (M2004-003), the Israeli Science Foundation (Grant 484/04), the Chief Scientist at the Israeli Ministry of Health (Grant 5807), and the Yedidut Research Grant.

Submitted for publication February 26, 2007; revised April 25, 2007; accepted July 2, 2007.

Disclosure: **A. Beit-Ya'acov**, None; **L. Meissonnier-Mizrahi**, None; **A. Obolensky**, None; **C. Landau**, None; **A. Blumenfeld**, None; **A. Rosenmann**, None; **E. Banin**, None; **D. Sharon**, None

The publication costs of this article were defrayed in part by page charge payment. This article must therefore be marked "advertisement" in accordance with 18 U.S.C. §1734 solely to indicate this fact.

Corresponding author: Dror Sharon, Department of Ophthalmology, Hadassah-Hebrew University Medical Center, Jerusalem, Israel; dror.sharon1@gmail.com.

The *ABCA4* (*ABCR*) gene encodes a retina-specific ATP-binding cassette (ABC) transport protein located at the rim of photoreceptor outer segment discs. The *ABCA4* protein belongs to the ABC transporters protein family and is involved in retinoid (*N*-retinylidene-phosphatidylethanolamine) transport across the disc membrane.<sup>1,2</sup>

Mutations in *ABCA4* cause a variety of retinal diseases.<sup>3-5</sup> *ABCA4* is the only gene known to cause autosomal recessive (AR) Stargardt disease (detection rate, 58%–78%).<sup>6,7</sup> Patients with Stargardt disease experience central visual loss in the first two decades of life, often with an initially normal fundus appearance. Later on, Stargardt disease is associated with macular atrophy and yellowish deep retinal flecks, while peripheral vision is largely preserved. Three different subtypes of Stargardt disease have been described based on electroretinal findings,<sup>8,9</sup> with group 3 the most severe phenotype in which peripheral retinal involvement occurs in addition to maculopathy. *ABCA4* mutations were also found in a few patients with AR retinitis pigmentosa, a progressive retinal degeneration that initially affects the rod photoreceptors but that ultimately also leads to gradual loss of cones. Mutations in *ABCA4* have also been identified in 30% to 50% of patients with AR cone-rod degeneration (CRD),<sup>5,10</sup> in which cones are initially affected and rod degeneration ensues. The involvement of *ABCA4* in age-related macular degeneration is still controversial, but accumulating data point to involvement in a small percentage of cases.<sup>11</sup>

We describe here a detailed clinical and genetic analysis of patients from six families residing in the same village who manifest a unique retinal degeneration caused by novel *ABCA4* mutations. In addition, we describe the existence of novel *ABCA4* transcripts, produced by alternative splicing, in the normal retina.

## PATIENTS AND METHODS

### Patients

This study, which involved human patients, conformed to the tenets of the Declaration of Helsinki and was approved by the institutional review board. Informed consent was obtained from the subjects after explanation of the nature and possible consequences of the study. DNA was purified from blood samples using the salting-out technique.<sup>12</sup>

### Clinical Evaluation

Full ophthalmologic examination, including assessment of visual acuity (VA), ocular motility, pupillary reaction, biomicroscopic slit-lamp, and dilated fundus examination, was performed in all patients. Subsequently, kinetic perimetry (Goldman visual fields, targets V<sub>4c</sub> and III<sub>4c</sub>), color vision testings, full-field electroretinography (ERG), and electrooculography (EOG) were performed.<sup>13</sup> Full-field ERGs were recorded using corneal electrodes and a computerized system (UTAS 3000; LKC, Gaithersburg, MD). In the dark-adapted state, a rod response to a dim blue flash and a mixed cone-rod response to a white

flash were acquired. Cone responses to 30-Hz flashes of white light were acquired under a background light of 21 cd/m<sup>2</sup>. All ERG responses were filtered at 0.3 to 500 Hz, and signal averaging was used. EOG was performed according to the International Society for Clinical Electrophysiology of Vision (ISCEV) standard using bilateral skin electrodes on both canthi, and the Arden ratio (light peak to dark trough) was derived.<sup>14</sup>

### ABCA4 Haplotype Analysis

DNA amplification was performed by 35 cycles consisting of denaturation at 94°C, annealing at 54°C, and extension at 72°C for 30 seconds each. In addition, an initial denaturation and final extension steps of 5 minutes each were performed. Haplotype analysis included four microsatellite markers (D1S435, D1S188, D1S2719, D1S497) flanking *ABCA4* and two single nucleotide polymorphisms (SNPs; rs472908 and rs560426 with 5 U NEB enzyme *Tsp509I* at 65°C and *Hpy188III* at 37°C, respectively) located within *ABCA4*. Restriction products were separated by electrophoresis in 3% agarose gel for 50 minutes.

### Mutation Analysis

The single-strand conformation polymorphism and direct sequencing techniques were used to screen all 50 coding exons of *ABCA4* (RefSeq NM\_000350.2). Screening for all known *ABCA4* sequence changes was performed at Asper Biotech using the *ABCA4* genotyping microarray (<http://www.asperophthalmics.com/ABCRgenetest.htm>).<sup>6</sup>

### Reverse Transcription and Nested PCR Analysis

We used a previously described protocol<sup>15</sup> to study *ABCA4* splicing. Total RNA was isolated from Epstein-Barr virus-transformed lymphoblastoid cells (RNeasy; Qiagen, Valencia, CA). RT-PCR was performed (Reverse-iT; Abgene, Epsom, UK) with random decamers, and cDNA amplification was performed with primers 737f (5'-aacgtcaacccccgacac-3') and 738r (5'-tctgtcctcagctcaggtcttg-3'). This was followed by a nested-PCR reaction with primers 351f (5'-ctacctgtgttttggctctg-3') and 257r (5'-actctggcagcagtgtag-3'). PCR products were gel purified and sequenced. We used the Splice-Site Prediction by Neural Network ([http://www.fruitfly.org/seq\\_tools/splice.html](http://www.fruitfly.org/seq_tools/splice.html)) for prediction of splice-site sequences.

## RESULTS

### Description of Pedigrees

Six reportedly unrelated Arab-Muslim families (Fig. 1A) residing in the same village who share a similar ocular phenotype were studied. Three of the families (MOL0006, MOL0033, and MOL0261) were large and included multiple consanguineous marriages. The inheritance pattern was interpreted as AR in all six families, with a pseudodominant inheritance pattern in MOL0006 because of multiple consanguineous marriages (Fig. 1A).

### Clinical Description

The ocular findings in early stages of disease in patients from the six families resemble those of typical Stargardt, mainly involving the macula, with a resultant reduction of central acuity and impaired color vision appearing toward the end of the first decade of life. Visual acuity (VA) was 6/9 in a 4-year-old patient and 6/18 in a 7-year-old patient, but after 10 years of age all patients had VA of 6/30 or worse, as is often the case in Stargardt disease. However, in all but one patient (MOL0006 I-2), the disease at later ages progressed to a severe, widespread retinal degeneration, beyond involvement of the macular region alone.

A representative example of the early stage of disease is patient MOL0033 II-4. At 14 years of age, her VA was 6/60, and yellow flecks and macular atrophy were evident (Fig. 2A).

Fluorescein angiography showed hyperfluorescence of the flecks and staining of atrophy in the macular region with a dark choroid effect in the background (Fig. 2B), characteristic of Stargardt disease. In older patients, however, large areas of atrophy and grayish discoloration of the retina were evident, with pigment migration and large pigment clumps in the posterior pole, midperiphery, and along the vessels (Figs. 2D-F). These findings suggest widespread retinal degeneration, beyond that usually associated with typical Stargardt disease. The progressive nature of the disease can be appreciated in the serial images of patient MOL0006 II-7 (Figs. 2G-I). At the age of 8, his VA was 6/30, and macular changes were slight (Fig. 2G). At the age of 12, his VA dropped to 6/60, and macular changes were more pronounced yet still compatible with typical Stargardt (Fig. 2H). However, at age 18 (VA 6/60), widespread retinal involvement was evident with atrophy and pigment clumps (Figs. 2I-L). Interestingly, autofluorescence imaging showed a relatively preserved parapapillary ring (Fig. 2K), as previously noted in patients with *ABCA4* mutations.<sup>16</sup>

Different measures of retinal function showed a similar pattern of progression over time, with initial macular involvement evolving into widespread retinal degeneration. The full-field cone-flicker ERG of MOL0006 II-2 (age 20) was delayed and amplitudes were still within normal limits (Fig. 3A), whereas the response of the foveal cones was severely reduced and delayed (Fig. 3B). Visual field testing of patient MOL0033 II-2 (age 20) showed that in addition to the central scotoma expected in Stargardt disease, there was also some narrowing of the visual fields (Fig. 3C), suggesting peripheral retinal involvement. Patient MOL0261 III-1 (Fig. 1A, age 25) is a representative example of the more advanced stage of disease. Mixed cone-rod and 30-Hz cone flicker full-field ERG amplitudes were reduced to approximately 50% of low threshold of normal (Fig. 3D), and cone flicker implicit time was markedly delayed (Fig. 3D, cone flicker waveforms; Fig. 4, other measures of retinal function [diamond correlating to age 25]). Fundus findings in this patient (age 29) indeed support widespread retinal involvement (Fig. 2E).

To better characterize the progress of disease and its association with age, we evaluated retinal function in 14 patients with the same retinal phenotype and genotype. The data presented in Figure 4 show a statistically significant decline in retinal function compared with age in most measures. Cone flicker amplitudes showed a trend of reduction with age, which did not attain statistical significance. In addition, in most patients who could undergo EOG, dysfunction of the retinal pigment epithelium was evident.

The only exception to this pattern of progression was patient MOL0006 I-2. At the age of 40, her fundus findings remained localized to the macular area, which had a typical Stargardt-like appearance (Fig. 2C). Full-field ERG function was maintained within normal limits, and EOG findings were at the lower limit of normal (Fig. 4, squares). This exception can be explained by the molecular genetic findings detailed below.

### Haplotype and Mutation Analysis

Given the retinal phenotype described and the inheritance pattern of the six families, we considered *ABCA4* the major candidate gene causative of the disease. Therefore, we performed haplotype analysis of families MOL0006 and MOL0033 using DNA markers located within and flanking the *ABCA4* gene (Fig. 1B). In family MOL0006, two different haplotypes, 1 and 3, cosegregated with the disease under the assumption of AR inheritance. Patient MOL0006 I-2 (diagnosed with typical Stargardt) carried both haplotypes, and her unaffected husband carried haplotypes 1 and 2; the latter did not cosegregate with the disease. All affected children, diagnosed with progressive,

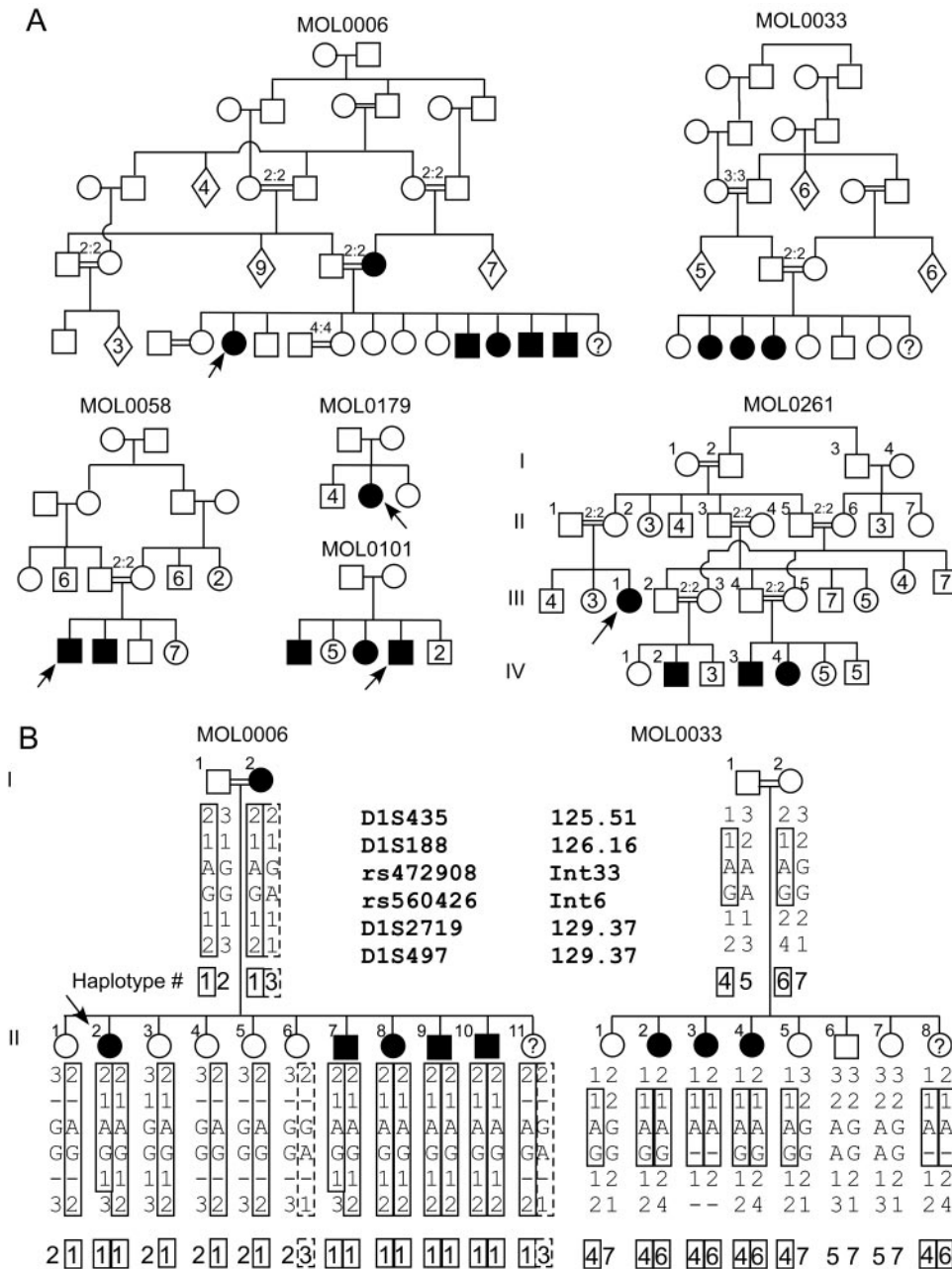


**FIGURE 1.** Family trees and haplotype analysis of the studied families. (A) Pedigrees of the six families included in the study, all residing in the same village. Family number is depicted above the corresponding family tree. Filled symbols represent patients. Open symbols represent unaffected family members. Numbers within open symbols represent the number of unaffected brothers (square), sisters (circle), or siblings of unspecified sex (diamond), and arrows indicate the proband. Double horizontal line represents consanguinity, with the number above it indicating the degree of consanguinity (for example, 2:2 indicates marriage between first cousins). (B) Haplotype analysis of families MOL0006 and MOL0033. Generation number (left) and an individual serial number (above each symbol) are depicted. Microsatellite and SNP markers are depicted according to their order on chromosome 1. Localization of the microsatellite markers based on the Marshfield map (as the distance in centimorgan) and SNP markers within *ABCA4* are presented. Each haplotype is numbered, and the segregating haplotypes (1, 3, 4, 6) are boxed.

severe Stargardt-like disease, were homozygote for haplotype 1. In family MOL0033, two haplotypes, 4 and 6, shared an identical portion within *ABCA4* and cosegregated with the disease. Moreover, haplotype 1, cosegregating in family MOL0006, shared the same *ABCA4* portion with haplotypes 4 and 6.

Based on these data, we assumed that two different *ABCA4* mutations were responsible for the two retinal phenotypes, one of which is shared by haplotypes 1, 4, and 6. To identify these mutations, we screened the DNA of two affected patients for all known *ABCA4* sequence variants by using the Asper biotech *ABCA4* mutation detection microarray.<sup>6</sup> The screen revealed seven sequence changes (c.1269C>T [p.His423His], c.1356+5delG, c.4773+48C>T, c.6069C>T [p.Ile2023Ile], c.6249C>T [p.Ile2083Ile], c.6285T>C [p.Asp2095Asp], and c.6764G>T [p.Ser2255Ile]) that had been previously interpreted as nonpathogenic changes. We subsequently performed mutation screening of the whole *ABCA4* open-reading-frame

and identified two previously reported nonpathogenic changes (c.6282+7G>A and c.302+26A>G) and a novel in-frame deletion (c.3449\_3451delGCT [p.Cys1150del]) in exon 23, found heterozygously in patient MOL0006 I-2 (Fig. 5A). The deleted amino acid (Cys1150) is highly conserved, resides within a conserved *ABCA4* region (Fig. 5A, bottom), and is located at the 3'-end of the ABC transporter nucleotide-binding domain. We could not identify this mutation in 190 chromosomes from healthy Arab-Muslim control subjects, nor could we find it in 30 unrelated Arab-Muslim patients with Stargardt disease or CRD. We considered it a pathogenic *ABCA4* mutation. We could not identify a second *ABCA4* mutation in our mutation analysis of the remaining exons, but we were consistently unable to amplify exon 29 by PCR using the DNA of patients with a diagnosis of progressive Stargardt-like disease. We performed a long-range PCR reaction and amplified the region encompassing exon 29. Sequencing analysis of this fragment revealed an intronic deletion of 23 nucleotides overlapping

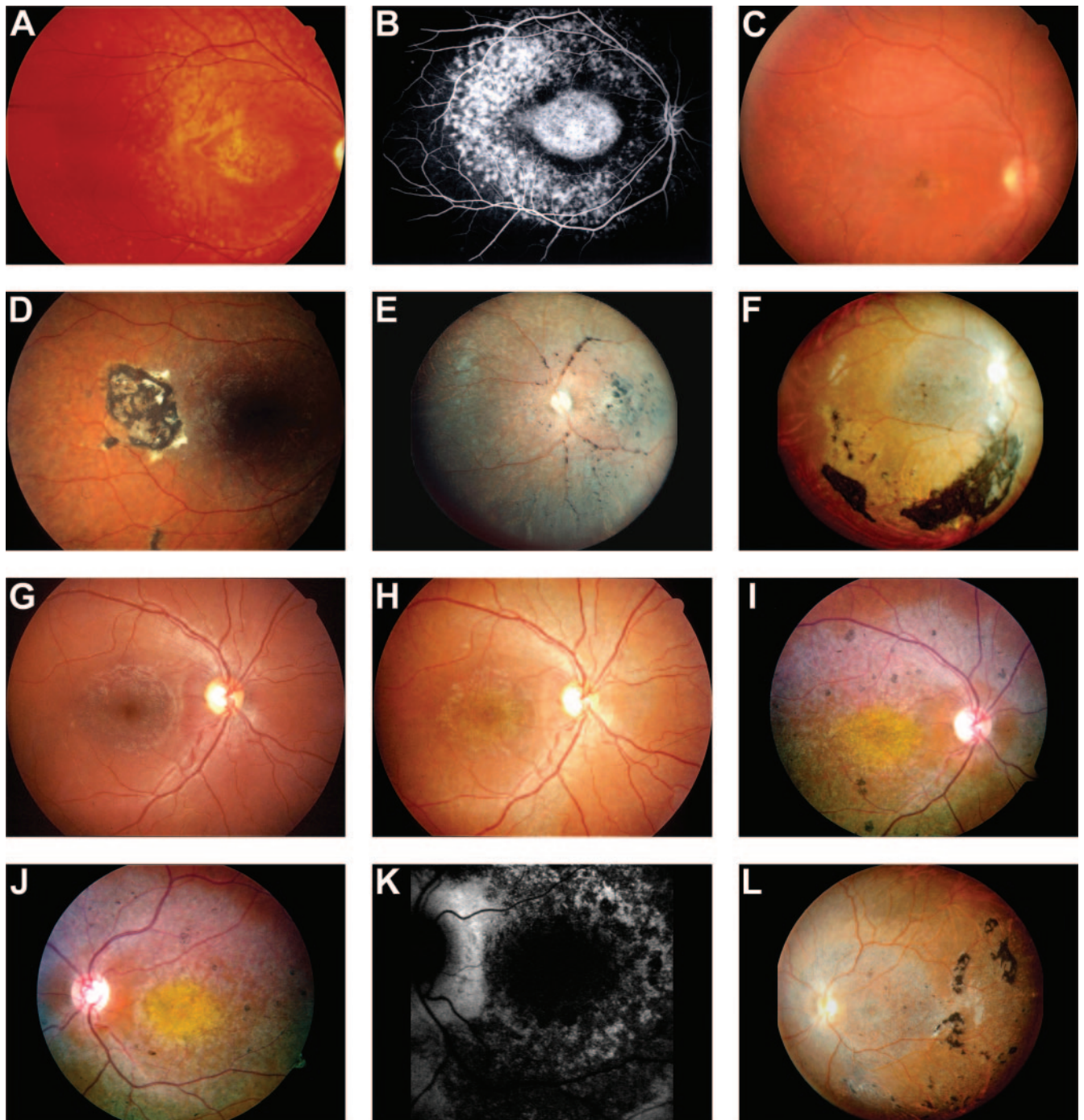


**FIGURE 2.** Fundusoscopic findings in patients from the six studied families. (A) Fundus photograph and (B) fluorescein angiography of patient MOL0033 II-4 at age 14, depicting the early stages of disease. Note the dark choroid effect on angiography. (C) Fundus photograph of patient MOL0006 I-2 (age 40) with typical Stargardt disease, without peripheral involvement (haziness of photograph caused by cataract). (D–F) Fundusoscopic findings in advanced stages of disease. Note widespread, often large pigment clumps. (D) MOL0006 II-2 at age 20. (E) MOL0261 III-1 at age 29. (F) MOL0261 IV-2 at age 22. (G–L) Fundusoscopic findings of patient MOL0006 II-7 at various ages: (G) 8 years; (H) 12 years (I–L) 18 years. (K) Autofluorescence image; note the relatively preserved parapapillary ring. (E, F, L) Panoret images.

with the forward primer of exon 29. The deletion (c.4254-15del23 [IVS28-15del23bp]) was located 15 bp upstream of exon 29 (Fig. 5B), and computer splice-site prediction analysis revealed a high score (0.83 of 1.00) for the wild-type acceptor site; the score for the mutant site was much lower (0.44 of 1.00). The mutation was shared by patients from all six families (Fig. 1) and was absent in 190 Arab-Muslim chromosomes of control subjects. Analysis of two SNP markers within the

*ABCA4* gene revealed a shared haplotype (rs472908-A and rs560426-G) in all affected patients who were homozygote for the c.4254-15del23 mutation.

#### Transcript Analysis

Two *ABCA4* transcripts have thus far been reported in normal retinal samples.<sup>3</sup> To explore the possibility that the c.4254-

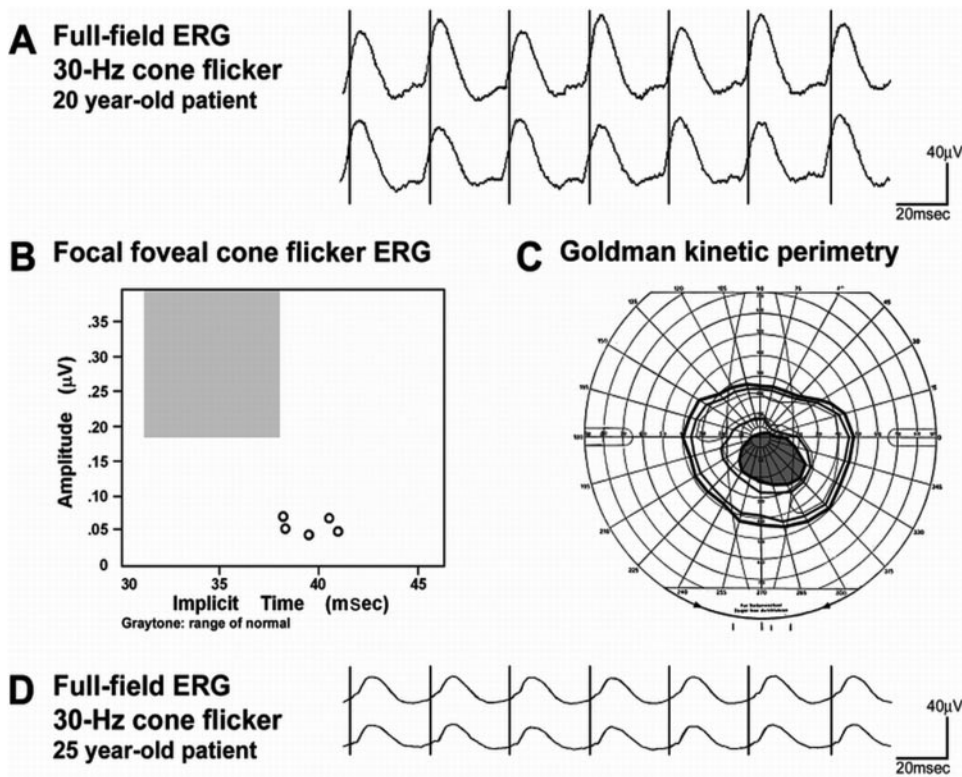


**FIGURE 3.** Retinal and macular function at different stages of disease. (A) Full-field cone flicker ERG is delayed, but amplitudes are still within normal limits in a 20-year-old patient (MOL0006 II-2). (B) In the same patient, focal foveal cone ERG response are already severely reduced and delayed (range of normal denoted by gray area). (C) Goldman kinetic perimetry in another 20-year-old patient (MOL0033 II-2) reveals narrowing of the visual fields in addition to a central scotoma, suggesting the beginning of peripheral retinal involvement. (D) In patient MOL0261 III-1, at the age of 25 years, full-field cone flicker ERG responses are markedly reduced, indicating involvement of extramacular cones.

15del23 mutation results in aberrant *ABCA4* splicing, we isolated total RNA from a normal retina and from Epstein-Barr virus-transformed lymphoblastoid cells of one control subject,

a heterozygote individual, and a homozygote patient. Surprisingly, the analysis of *ABCA4* exons 27 to 31 in the normal retina yielded four different transcripts (Table 1; Fig. 5C). The

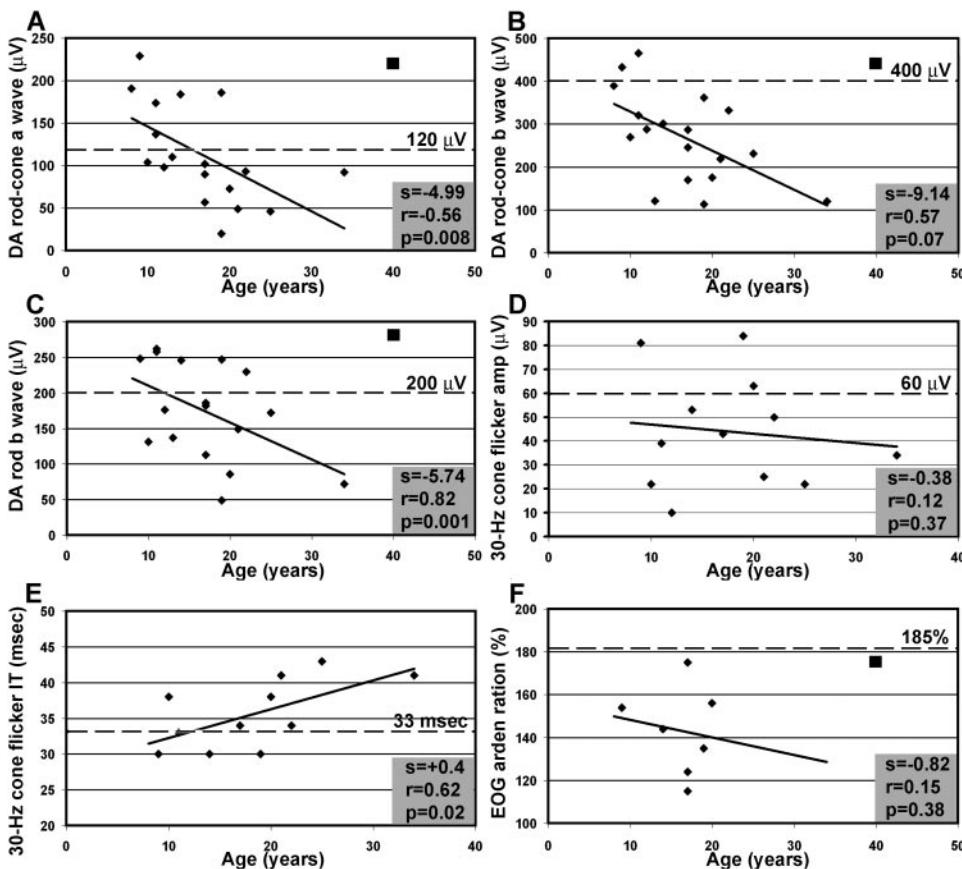


**FIGURE 4.** Retinal function as measured by full-field electroretinography (FFERG) deteriorates with age in patients who are homozygote for the c.4254-15del23 *ABCA4* mutation (diamonds). The patient, who is a compound heterozygote for the c.4254-15del23 and p.Cys1150del mutations (square), has relatively preserved responses even at age 40. (A) Dark-adapted FFERG mixed rod-cone response a-wave amplitudes. (B) Dark-adapted FFERG mixed rod-cone response b-wave amplitudes. (C) Dark-adapted FFERG rod response b-wave amplitudes. (D) Light-adapted FFERG 30-Hz cone flicker amplitude. (E) Light-adapted FFERG 30-Hz cone flicker implicit time. (F) Electrooculogram Arden ratio. The value for each patient is the average between the right and the left eyes. Regression lines were fitted by least-squares analysis. Lower limit of normal for amplitudes and upper limit for implicit time are marked by dotted lines.

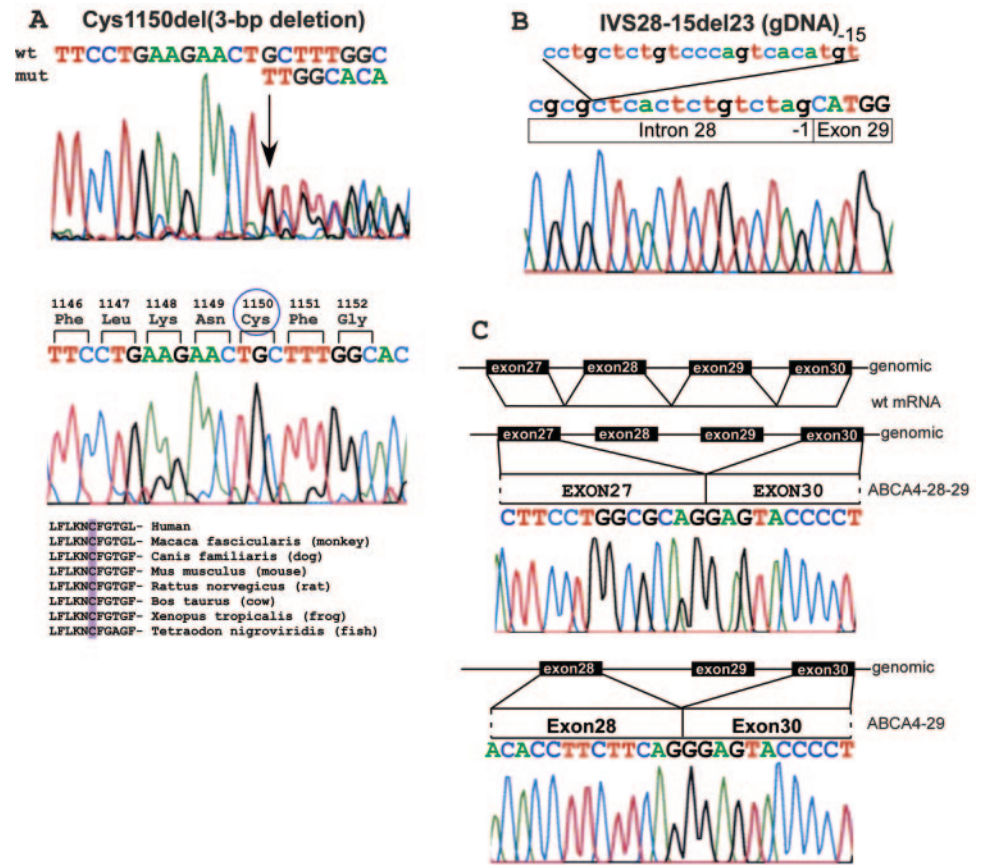


**FIGURE 5.** Novel *ABCA4* mutations and transcripts. (A) Chromatograms showing the sequence around p.Cys1150 in patient MOL0006 I-2, who is heterozygote for the p.Cys1150del mutation because of a deletion of 3 bp (GCT) in exon 23 (*upper panel*) and a wild-type sequence (*lower panel*). The arrow points to the deletion site. An alignment of this region in orthologous *ABCA4* sequences is presented below the chromatograms. Note that Cys1150 is conserved in all species. (B) Chromatograms showing the intron-exon junction in patient MOL0006 II-2, who is homozygote for the c.4254-15del23 mutation. The 23 deleted bases are depicted above the mutant sequence. Intronic sequence is presented in lowercase and exonic sequence in uppercase. (C) Alternative-spliced transcripts in *ABCA4*. The wild-type *ABCA4* transcript and two novel alternatively spliced isoforms (*ABCA4-28-29* and *ABCA4-29*) are depicted.

normal *ABCA4* transcript, including exons 27 through 31 (*ABCA4\_v1*), had the highest expression level. An aberrant transcript, in which exons 28 and 29 were skipped (*ABCA4\_v2*) causing a frameshift deletion of 224 nucleotides, showed a relatively high expression level (75% of the wild-type expression). Two additional transcripts were in-frame and were expressed at relatively low levels. Exon 29 was skipped in *ABCA4\_v3* (expression level 9%, comparing to the wild-type transcript), causing a deletion of 99 nucleotides. Exon 29 and the first 114 nucleotides of exon 30 were skipped in *ABCA4\_v4* (15% of the wild-type expression level). A transcript similar to that of *ABCA4\_v4* was the first *ABCR* transcript to be reported.<sup>3</sup> It contains exon 29 but not the first 114 nucleotides of exon 30.<sup>3,4</sup> Although full-length exons were included or deleted in transcripts *ABCA4\_v1* to 3, transcript *ABCA4\_v4* contained only part of exon 30. Sequence analysis of this exon supported previous findings<sup>4</sup> that identified a cryptic acceptor splice site located 114 nucleotides within exon 30 (a predicted splice-site score of 0.91). These transcripts were identified in normal retina and in lymphoblastoid cells from the healthy control subject and the heterozygote patient. Detailed RT-PCR analysis of the homozygote patient revealed only the three alternatively spliced isoforms, whereas the full-length *ABCA4* transcript could not be detected.

## DISCUSSION

The present study describes the involvement of two novel *ABCA4* mutations in retinal degenerative disease of differing severity. The p.Cys1150del mutation results in a deletion of a highly conserved amino acid located 3' to the ABC transporter nucleotide-binding domain. It was found heterozygously in one patient (MOL0006 I-2) with the diagnosis of Stargardt disease. The founder mutation, c.4254-15del23, causes a splicing defect resulting in the absence of the wild-type *ABCA4* transcript. This mutation was found homozygously in 14 patients who manifested progressive Stargardt-like disease and heterozygously in patient MOL0006 I-2.

More than 500 *ABCA4* mutations have been identified as causing different retinal diseases, allowing a proposed genotype-phenotype correlation model.<sup>4,5,17</sup> The simplified model suggests that patients with two severe mutations have retinitis pigmentosa, patients with one severe and one moderate mutation have CRD, patients with one severe and one mild mutation have Stargardt disease, and patients with only one severe or moderate mutation are at increased risk for age-related macular degeneration. As can be expected, actual genotype-phenotype correlations are more complex, and deviations from this model have been reported.<sup>5,17,18</sup> Interestingly, as in the homozygote patients de-

**TABLE 1.** *ABCA4* Retinal Transcripts

Transcript	Exons Included	Exons Skipped	Effect on ORF	Relative Expression Level
<i>ABCA4_v1</i>	wt (27-31)	None	None	1.00
<i>ABCA4_v2</i>	27,30,31	28,29	-224 bp frameshift	0.75
<i>ABCA4_v3</i>	27,28,30,31	29	-99 bp in-frame	0.09
<i>ABCA4_v4</i>	27,28,30p,31	29,30p	-213 bp in-frame	0.15

scribed here, progression from an initially mild, characteristic phenotype to a severe one, usually CRD, may also occur over time.<sup>18-20</sup>

The major limitation in obtaining an accurate genotype-phenotype correlation model is the correct interpretation of the effect of a given mutation on protein structure or function. This is particularly difficult with potential splicing mutations, which can lead to mild or severe mutations. Analysis of such mutations is challenging because of technical difficulties in amplifying *ABCA4* mRNA from readily available tissues, such as peripheral blood and lymphoblastoid cells.<sup>4</sup> In only one study thus far<sup>15</sup> has reliable splicing data been obtained through this system, leading to an unexpected result: a frequent base substitution (c.2588G>C) in the first base of exon 17, initially interpreted as a missense mutation (Gly863Ala), created a splicing defect, resulting in a deletion of one amino acid (Gly863). This result emphasizes the importance of accurate mRNA analysis for each suspected splicing mutation before any genotype-phenotype assumptions can be made. Our nested RT-PCR analysis of the retina and lymphoblastoid cells revealed an unexpected result. We found that *ABCA4* produced four different transcripts in the normal retina through an alternative-splicing mechanism. The two most common transcripts are the wild-type *ABCA4* mRNA and a variant (*ABCA\_v2*) in which exons 28 and 29 are skipped. This deletion causes a frameshift and is therefore likely to be recognized and degraded by the nonsense mediated decay (NMD) mechanism.<sup>21</sup> The other two transcripts (*v3* and *v4*) have in-frame deletions and are expressed at very low levels, probably producing low amounts of nonfunctional *ABCA4* proteins. The splicing region of all five *ABCA4* transcripts described thus far (the wild-type transcript, a splicing variant with part of exon 30 as reported previously,<sup>3,4</sup> and three additional splice variants reported here) is located between exons 28 and 30 of the *ABCA4* gene. Interestingly, this region contains a number of cryptic splice sites<sup>4</sup> and a few splice-site mutations. The novel splicing mutation we identified in this study, c.4254-15del23, prevents the production of the wild-type *ABCA4* protein and is likely to be a null mutation. However, we cannot exclude the possibility that small amounts of the wild-type protein are still translated in the retinas of these patients. If such a low level of expression indeed exists, it may explain the delayed appearance of widespread retinal degeneration in our patients compared with other patients who manifest early, full-blown CRD or retinitis pigmentosa because of homozygosity for null *ABCA4* mutations.

### Acknowledgments

The authors thank Dvorah Abeliovich, Aviva Yechezkel, and Ruhama Neis for technical assistance and Alessandra Maugeri for advice and technical help regarding the RT-PCR analysis.

### References

- Beharry S, Zhong M, Molday RS. N-retinylidene-phosphatidylethanolamine is the preferred retinoid substrate for the photoreceptor-specific ABC transporter *ABCA4* (ABCR). *J Biol Chem*. 2004; 279:53972-53979.
- Higgins CF. ABC transporters: from microorganisms to man. *Annu Rev Cell Biol*. 1992;8:67-113.
- Allikmets R, Singh N, Sun H, et al. A photoreceptor cell-specific ATP-binding transporter gene (ABCR) is mutated in recessive Stargardt macular dystrophy (published correction appears in *Nat Genet*. 1999;17:122). *Nat Genet*. 1997;15:236-246.
- Cremers FP, van de Pol DJ, van Driel M, et al. Autosomal recessive retinitis pigmentosa and cone-rod dystrophy caused by splice site mutations in the Stargardt's disease gene ABCR. *Hum Mol Genet*. 1998;7:355-362.
- Maugeri A, Klevering BJ, Rohrschneider K, et al. Mutations in the *ABCA4* (ABCR) gene are the major cause of autosomal recessive cone-rod dystrophy. *Am J Hum Genet*. 2000;67:960-966.
- Jaakson K, Zernant J, Kulm M, et al. Genotyping microarray (gene chip) for the *ABCR* (*ABCA4*) gene. *Hum Mutat*. 2003;22:395-403.
- Rivera A, White K, Stohr H, et al. A comprehensive survey of sequence variation in the *ABCA4* (ABCR) gene in Stargardt disease and age-related macular degeneration. *Am J Hum Genet*. 2000;67:800-813.
- Lois N, Holder GE, Bunce C, Fitzke FW, Bird AC. Phenotypic subtypes of Stargardt macular dystrophy-fundus flavimaculatus. *Arch Ophthalmol*. 2001;119:359-369.
- Gass JDM. *Stereoscopic Atlas of Macular Diseases: Diagnosis and Treatment*. 4th ed. St. Louis: Anne S. Patterson; 1997.
- Birch DG, Peters AY, Locke KL, et al. Visual function in patients with cone-rod dystrophy (CRD) associated with mutations in the *ABCA4*(ABCR) gene. *Exp Eye Res*. 2001;73:877-886.
- Allikmets R. Further evidence for an association of ABCR alleles with age-related macular degeneration: the International ABCR Screening Consortium. *Am J Hum Genet*. 2000;67:487-491.
- Miller SA, Dykes DD, Polesky HF. A simple salting out procedure for extracting DNA from human nucleated cells. *Nucleic Acids Res*. 1988;16:1215.
- Banin E, Shalev RS, Obolensky A, et al. Retinal function abnormalities in patients treated with vigabatrin. *Arch Ophthalmol*. 2003; 121:811-816.
- Marmor MF, Zrenner E. Standard for clinical electro-oculography: International Society for Clinical Electrophysiology of Vision. *Arch Ophthalmol*. 1993;111:601-604.
- Maugeri A, van Driel MA, van de Pol DJ, et al. The 2588G>C mutation in the *ABCR* gene is a mild frequent founder mutation in the Western European population and allows the classification of ABCR mutations in patients with Stargardt disease. *Am J Hum Genet*. 1999;64:1024-1035.
- Cideciyan AV, Swider M, Aleman TS, et al. *ABCA4*-associated retinal degenerations spare structure and function of the human parapapillary retina. *Invest Ophthalmol Vis Sci*. 2005;46:4739-4746.
- Gerth C, Andrassi-Darida M, Bock M, et al. Phenotypes of 16 Stargardt macular dystrophy/fundus flavimaculatus patients with known *ABCA4* mutations and evaluation of genotype-phenotype correlation. *Graefes Arch Clin Exp Ophthalmol*. 2002;240:628-638.
- Simonelli F, Testa F, Zernant J, et al. Association of a homozygous nonsense mutation in the *ABCA4* (ABCR) gene with cone-rod dystrophy phenotype in an Italian family. *Ophthalmic Res*. 2004; 36:82-88.
- Klevering BJ, Deutman AF, Maugeri A, Cremers FP, Hoyng CB. The spectrum of retinal phenotypes caused by mutations in the *ABCA4* gene. *Graefes Arch Clin Exp Ophthalmol*. 2005;243:90-100.
- Klevering BJ, van Driel M, van de Pol DJ, et al. Phenotypic variations in a family with retinal dystrophy as result of different mutations in the *ABCR* gene. *Br J Ophthalmol*. 1999;83:914-918.
- Hentze MW, Kulozik AE. A perfect message: RNA surveillance and nonsense-mediated decay. *Cell*. 1999;96:307-310.